Glacier velocities and dynamic ice discharge from the Queen Elizabeth Islands, Nunavut, Canada

Wesley Van Wychen[1,2], David O. Burgess[2], Laurence Gray[1], Luke Copland[1], Martin Sharp[3], Julian A. Dowdeswell[4], and Toby J. Benham[4]

(1) Department of Geography, University of Ottawa, Ottawa, Ontario, Canada K1N 6N5 (wvanw046@uottawa.ca)

(2) Natural Resources Canada, Geological Survey of Canada, 601 Booth St., Ottawa, Ontario, Canada K1A 0E8

(3) Department of Earth and Atmospheric Sciences, University of Alberta, Edmonton, Alberta, Canada T6G 2E3

(4) Scott Polar Research Institute, University of Cambridge, Lensfield Road, Cambridge, UK CB2 1ER, UK

This article has been accepted for publication and undergone full peer review but has not been through the copyediting, typesetting, pagination and proofreading process which may lead to differences between this version and the Version of Record. Please cite this article as doi: 10.1002/2013GL058558

Abstract:

Recent studies indicate an increase in glacier mass loss from the Canadian Arctic Archipelago as a result of warmer summer air temperatures *[Gardner et al., 2011]*. However, no complete assessment of dynamic ice discharge from this region exists. We present the first complete surface velocity mapping of all ice masses in the Queen Elizabeth Islands, and show that these ice masses discharged ~2.6 ± 0.8 Gt a^{-1} of ice to the oceans in winter 2012. ~50% of the dynamic discharge was channelled through non surge-type Trinity and Wykeham Glaciers alone. Dynamic discharge of the surge-type Mittie Glacier varied from 0.90 ± 0.09 Gt a^{-1} during its 2003 surge to 0.02 ± 0.02 Gt a^{-1} during quiescence in 2012, highlighting the importance of surge-type glaciers for inter-annual variability in regional mass loss. Queen Elizabeth Islands glaciers currently account for ~7% of reported dynamic discharge from Arctic ice masses outside Greenland.

Key Points:

- Surface velocities of ice masses in the Queen Elizabeth Islands are mapped
- Dynamic discharge is estimated and its importance to total mass loss assessed
- Queen Elizabeth Islands dynamic discharge is compared with other Arctic regions

1.0 Introduction and Study Area

The Queen Elizabeth Islands (QEI; Devon, Ellesmere and Axel Heiberg Islands; Fig 1 inset) contain ~104,000 km^2 of glacier ice, which represents 25% of Arctic glacier ice outside the Greenland Ice Sheet *[Arendt et al., 2012]*. Long-term surface mass balance records from this region indicate that prior to the late 1980s the ice masses were largely in balance *[Koerner, 2005; Mair et al., 2009; Sharp et al., 2011]*. Since the late 1980s however, and especially since 2005, changing summer atmospheric circulation patterns have increased advection of warm air from the northwest Atlantic to the Canadian High Arctic, leading to increased surface melt, longer melt seasons and increased anti-cyclonic air circulation over the QEI in summer *[Gardner et al., 2011; Sharp et al., 2011; Lenaerts et al., 2013]*. As a consequence, ice loss from the QEI via surface mass balance has increased sharply in recent years (averaging -7 ± 18 Gt a^{-1} between 2004-2006, and -61 ± 18 Gt a^{-1} between 2007-2009) *[Gardner et al., 2011]*. However, little is known about the importance of dynamic discharge as a mass loss mechanism in the QEI. This study provides the first complete mapping of surface velocities of all ice masses in the QEI and combines this with estimates of ice thickness near the termini of tidewater glaciers to estimate dynamic ice discharge to the ocean. Here we define dynamic ice discharge as the mass of ice passing through a terminus flux gate (also called iceberg flux in some studies); we do not account for the effects of terminus advance or retreat on dynamic ice discharge.

2.0 Methods

2.1 Determination of Surface Motion

Ice surface motion was determined using a custom written MATLAB speckle-tracking algorithm applied to Radarsat-2 fine beam (resolution; ~8 x 8 m) and ultrafine beam (resolution; ~3 x 3 m) imagery acquired in 24-day pairs between January and May 2012

(Supplementary Information Table 1). This algorithm tracks the relative displacement of small image chips by applying a two-dimensional cross-correlation algorithm to accurately co-registered Radarsat-2 image pairs (co-registration was completed using an area cross-correlation technique; *Gray et al. [2001]*). This method has previously proved effective for measuring surface ice displacements at the ice cap scale within the Canadian High Arctic *[Short and Gray, 2004, 2005; Van Wychen et al., 2012]*. Image acquisitions were restricted to mid- to late-winter due to the requirement for good coherence (e.g., little surface melt or snowfall) between scenes. Displacements were determined in both azimuth and range directions using chip sizes of ~450 m in azimuth and ~350 m in range for fine beam imagery and ~150 m in azimuth and ~125 m in range for ultrafine imagery. The 1:250 000 version of the Canadian Digital Elevation Dataset (CDED), Level 1, was used to remove the topographic component of the slant-range displacement. To remove systematic biases due to inaccuracies in the baseline or squint effects between image acquisitions, displacements were calibrated using manually selected areas of known zero motion, such as bedrock outcrops, to determine the local bias, which was then removed from the rest of the dataset *[Gray et al., 2001]*. Final displacements were converted to annual velocities. Displacement editing and filtering of the displacements followed the criteria of *Van Wychen et al., [2012]*: (1) surface ice velocities should be faster along glacier centrelines than at glacier margins; (2) flow direction should follow topography and surface flow features; and (3) flow vectors should not deviate dramatically from adjacent vectors in direction or magnitude over short distances. Filtering was performed manually using ArcGIS™ 9.2 and incorrect matches were removed from the dataset. The point velocity results were interpolated to 100 m grid spacing for the entire glaciated region of the QEI using an inverse distance-weighting method with a fixed 500 m search radius.

Output raster grids were mosaicked to produce a single velocity map for each major ice cap. In areas where rasters overlapped, the minimum overlapping value was used to provide a conservative estimate of ice velocity. To assess the consistency between results determined from different image pairs, we compared the absolute difference between overlapping raster pixels at ~6 million locations and determined a mean difference of 5.95 m a^{-1} and standard deviation of 15.5 m a^{-1}. The final raster was clipped using glacier outlines provided in version 3.0 of the Randolph Glacier Inventory (RGI) *[Arendt et al., 2012]* for the Canadian High Arctic. Due to our use of winter imagery, which does not capture summer speed-up events, we assume that velocity maps and calculated discharges represent minimum annual estimates. Comparison of continuous summer and winter dGPS records from the terminus region of the tidewater terminating Belcher Glacier, Devon Ice Cap, indicates that extrapolation of winter only velocities may underestimate annual velocities by ~10-15%. [B. Danielson, Personal Communication, Oct. 2013].

To establish motion errors, we assumed that the mean velocity calculated over marginal bedrock outcrops provides information about the error limits of the method. Based on a total of ~11 million measurements, mean displacement over bedrock was 5.9 m a^{-1} with a standard deviation of 6.3 m a^{-1} (error for individual ice masses is presented in Supplementary Information Table 2). To determine error throughout the interior regions of ice caps, where bedrock control was not available, displacements were extracted along ice divides where surface motion should be nearly zero *[Raymond, 1984]*. Major ice divides were derived from version 3.0 of the RGI and are shown as white lines in Figure 1. Mean velocities along ice divides provided an overall mean error of 6.8 m a^{-1} and standard deviation of 3.9 m a^{-1} (Supplementary Information Table 2).

2.2 Calculation of Dynamic Ice Discharge

This study utilizes airborne-radar measurements of ice thickness collected by NASA's Operation Icebridge campaigns over the Canadian High Arctic in May 2012 (for 56% of glaciers) and 2006 (5% of glaciers) *[Gogineni, 2012]*, the Scott Polar Research Institute in 2000 (32% of glaciers) *[Dowdeswell et al., 2004]*, and by the University of British Columbia in 1981 (5% of glaciers) *[Narod et al., 1988]*. The fluxgate for the Good Friday Bay Glacier on Axel Heiberg Island is located ~20 km from the calving front, and uses a centreline ice thickness estimated using an area-depth scaling scheme *[Ommanney, 1969]*. This is the only glacier that relies on this dataset, and is ascribed a 40% uncertainty based on comparison of ice thickness estimates provided by *Ommanney [1969]* for 4 different locations on Axel Heiberg Island with nearby (within 1.5 km) ice thickness measurements from NASA's Operation Icebridge in 2006.

To calculate dynamic ice discharge, both cross-section (20 of 41 glaciers, primarily located on Devon Ice Cap) and centreline methods (21 of 41 glaciers) were used depending on the availability of ice thickness datasets (Supplementary Information Table 1). For glaciers with depth measurements acquired perpendicular to ice flow, the cross-section method was used. In such cases, the terminus width was divided into a number of evenly spaced columns depending on the spacing between ice thickness data points unique to each acquisition and post-processing method (typically 20 – 30 m). For each column, upper and lower estimates of ice flux were calculated by assuming different fractional contributions of internal ice deformation to the measured surface velocity. For the lower ice flux estimate (Q_{min}) we assume a depth-averaged velocity of 80% of the measured surface velocity (i.e., 20% of the overall motion is accounted for by internal deformation) *[Paterson, 1994]*. For the upper estimate (Q_{max}) we assume that the depth averaged velocity is equal to the surface velocity,

and that ice movement is by basal sliding alone. Discharge was then calculated for each column width (W) using:

$$Q_{min} = (0.8 *(V - V_{error})) * (H - H_{error} + (T*E)) * (W) \quad (1)$$

$$Q_{max} = (V + V_{error}) * (H + H_{error} + (T*E)) * (W) \quad (2)$$

where V is surface ice velocity, V_{error} is a constant error derived separately for each ice mass from the velocity errors computed along ice divides (i.e., highest measured error as indicated in Supplementary Information Table 2), H is measured ice thickness, H_{error} is the error associated with each individual ice thickness dataset (Supplementary Information Table 1), T is the average annual terminus elevation change as determined from ICESat data in the QEI between 2003 and 2009 *[Gardner et al., 2011]* and E is the number of elapsed years between the acquisition of the ice thickness data and 2012. The ICESat dataset is the most complete elevation change dataset available for this region, and enables a correction to be made for the change in ice thickness between the time an ice thickness measurement was made and 2012. Total Q_{min} and Q_{max} for a cross section were then calculated from the sum of the individual column widths and provide error limits on our estimates.

For glaciers for which only centreline measurements of ice thickness were available, the cross sectional flux gate was assumed to have a "U" shape, based on the morphology of tidewater glaciers in the QEI for which cross-sections are known (e.g. *Gogineni, [2012]*) and modelling of valley form after long periods of erosion [*Harbor, 1992*]. This "U" shape was modelled based on:

$$H_{interpolated} = ((10 - C) / (D_1^2)) * (D_2^2) + C \quad (3)$$

where $H_{interpolated}$ is the assumed ice thickness using a parabolic interpolation from the measured ice thickness at the centreline to a marginal ice thickness of 10 m, C is the measured centreline ice thickness, D_1 is the distance from the centreline to the glacier margin and D_2 is the distance from the centreline to the centre of the interpolated ice column. Ice column thickness was interpolated at 20 m intervals from the centreline to the margins. To assess the quality of the modelled cross-sectional glacier geometries, we determined the difference between true glacier cross-sectional geometry and the cross-sectional geometry modelled from only a single point at the glacier centreline for all glaciers within the QEI with depth measurements collected perpendicular to ice flow. This analysis indicated that the centreline method of cross-sectional area modelling underestimated the true cross-sectional area by ~12%. We therefore multiply the modeled cross-sectional area by 1.12 to correct for this bias. Minimum and maximum discharges for each column were then calculated from:

$$Q_{min} = (0.8 *(V - V_{error})) * ((H_{interpolated} * 1.12) - H_{error} - (T*E)) * (W) \quad (4)$$

$$Q_{max} = (V + V_{error}) * ((H_{interpolated} * 1.12) + H_{error} + (T*E) * (W) \quad (5)$$

Total Q_{min} and Q_{max} for a cross section were calculated from the sum of the individual column fluxes and provide error limits on our estimates. Reported dynamic ice discharge values are the average of Q_{min} and Q_{max}, with Q_{min} and Q_{max} providing the lower and upper uncertainty bounds respectively.

3.0 Results and Discussion

Glacier velocities in the Queen Elizabeth Islands are generally relatively low (Figure 1 and Supplementary Figures 1 to 7). In the interior regions of ice caps and icefields, surface velocities are typically < 10 m a^{-1}, indicative of ice frozen to its bed and moving by ice deformation alone. Most tidewater glaciers have velocities of ~30 – 90 m a^{-1} (interquartile range) along their main trunks, rising to < 300 m a^{-1} at the terminus, while land-terminating glaciers typically have velocities ~20 - 50 m a^{-1} (interquartile range) along their main trunk, rising to < 75 m a^{-1} near the glacier terminus. For land-terminating glaciers, this pattern is different to the peak in velocity that is typically expected near the ELA, and could be due to the fact that these glaciers tend to have large accumulation areas that drain into relatively narrow valleys, and/or because they change from cold-based to warm-based between their accumulation and ablation areas *[Burgess et al., 2005; Copland et al., 2003a]*. The only tidewater glaciers with observed velocities > 300 m a^{-1} are the Belcher and Fitzroy Glaciers (located in the northeast sector of Devon Ice Cap (DIC)), and the Trinity and Wykeham Glaciers (located in the south-eastern region of Prince of Wales (POW) Icefield, Ellesmere Island). Short and Gray [2005] determined velocities of ~800 m a^{-1} at the terminus of Trinity Glacier and ~400 m a^{-1} at the terminus of Wykeham Glacier in 2004, which compare to our velocities of ~1200 m a^{-1} and ~500 m a^{-1}, respectively, in 2012. This suggests a recent flow acceleration, although the moderate velocity increase and lack of other evidence (e.g., looped moraines, new crevassing) suggests that this is unlikely due to surging. The higher velocities of these four glaciers may reflect relatively high local accumulation rates due to proximity to year-round moisture sources in the North Open Water Polynya and Baffin Bay *[Mair et al., 2009, Koerner, 1979]*.

Copland et al., [2003b] determined velocities of 1000 m a^{-1} along the whole 25 km length of

Mittie Glacier in 1999 and *Short and Gray [2005]* determined flow speeds of up to ~1000 m a^{-1} at the terminus of Mittie Glacier in winter 2003 and ~700 m a^{-1} in 2004. By comparison, we measured velocities that were < 10 m a^{-1} in 2012. This indicates that between 2004 and 2012 Mittie Glacier entered the quiescent phase of its surge cycle, and that its surge cycle is at least 5 years in length (and possibly longer). Similarly, the main trunk of Iceberg Glacier, Axel Heiberg Island, was flowing ~100 m a^{-1} in winter 2004 [Short and Gray, 2005] but was stagnant in 2012. Conversely, velocities determined in 2012 at the front of Good Friday Bay Glacier on southern Axel Heiberg Island are similar to those determined in the 1950s when the glacier was actively surging [Müller, 1969; Copland et al., 2003], suggesting that this glacier is currently in an active surge phase (although it only has a small impact (0.09 Gt a^{-1}) on total regional dynamic ice discharge even when surging). Only two land-terminating glaciers in the QEI have surface velocities exceeding 75 m a^{-1} (Chapman, Unnamed6), both of which have previously been identified as surge-type [Copland et al., 2003; Hattersley-Smith, 1969].

Fast flowing glaciers in the QEI (including surge-type glaciers) typically occupy deep subglacial troughs that channel flow from the upper reaches of the accumulation area towards the margins [Burgess et al. 2005]. Faster flowing glaciers tend to be located in areas of higher accumulation *[Koerner, 1979]* and occupy deeply incised terrain, such as is found on eastern DIC, eastern POW, and western Axel Heiberg Island. In contrast, slower flowing ice occurs in areas of lower accumulation *[Koerner, 1979]* and where glaciers overlie plateau-like surfaces, such as western DIC, western POW and eastern Axel Heiberg Island.

Total ice discharge from QEI glaciers is currently 2.6 ± 0.8 Gt a^{-1} (supplementary information Table 1). Ice discharge estimates reported here are similar to previous estimates from studies

of selected glaciers within this region *[Van Wychen et al., 2012; Short and Gray, 2005; Mair et al., 2009; Williamson et al., 2008; Burgess et al., 2005]*. A limited number of glaciers account for most of the ice discharge from the QEI and ~50% of total ice flux is channelled through just the Trinity and Wykeham Glaciers that drain POW Icefield (although this value likely varies temporally due to the frequent occurrence of tidewater glacier surging, or other forms of velocity variability, in the QEI). Similarly, a small number of glaciers typically dominate the discharge to the ocean from individual ice masses: Belcher and Fitzroy Glaciers (~55% of DIC), Cañon Glacier (~55% from Agassiz Ice Cap), Otto and Yelverton Bay Glaciers (~80% from Northern Ellesmere Icefields) and Good Friday Bay Glacier (~95% from Steacie and Müller Ice Caps). As a consequence, overall ice discharge to the ocean from the QEI may be highly sensitive to changes in the dynamics of only a few glaciers. To assess this, we combine the 2003 surge speeds of Mittie Glacier *[Short and Gray, 2005]* with our ice depth measurements to compute that in 2003 the Mittie Glacier would have contributed 0.90 ± 0.09 Gt a^{-1} of ice to the ocean, compared to 0.02 ± 0.02 Gt a^{-1} in 2012. This rapid change in ice flux from a single glacier signifies the importance of surge-type glaciers within the region, which may oscillate between being large and negligible contributors to dynamic ice discharge over relatively short periods (<10 years).

Comparison of our estimate of dynamic discharge with recent estimates of surface mass balance in the QEI provides insight into their relative importance to mass loss (assuming that the dynamic discharge in 2012 is representative of long term values). The 2012 discharge rates are equivalent to ~3.1% (2.6 vs. 83.3 Gt a^{-1}) of the average total annual runoff ((melt + rain) – refreezing) from the QEI from 2007-2009, the most recent period for which data are available *[Gardner et al., 2011; A. Gardner, Personal Communication, Dec. 2013]*. For the 2004-2006 period, the dynamic discharge would have been equivalent to ~5.2% (2.6 vs. 49.6

Gt a^{-1}) of the average total annual runoff. This suggests that current mass loss in the QEI is dominated by surface melt and run-off, and that dynamic discharge has become a proportionally smaller component of mass loss in recent years. Determining how ice discharge rates within the region may respond to this increase in surface melt and runoff requires further study.

To put the ice discharge rates reported here within a broader context, we compare our estimates with those for other Arctic glaciers and ice caps (GIC) outside of Greenland (Table 1). The QEI currently contributes ~7.1% of total reported dynamic ice discharge from GIC in the Arctic, although the exclusion of Greenland GICs (due to lack of flux data) means that this is likely an over-estimate. Nevertheless, Alaska and Svalbard account for the majority of mass loss via dynamic discharge currently reported for the circumpolar Arctic. The large differences in discharge are probably driven by regional variations in accumulation and climate, with more maritime regions experiencing higher rates of mass turnover and thus higher discharge rates (e.g., Alaska, precipitation ~1-5 m w.e. a^{-1}) *[Braithwaite, 2005]*), while more continental climates experience lower rates of mass turnover and relatively lower discharge (e.g., Canadian High Arctic, precipitation <0.5 m w.e. a^{-1} *[Braithwaite, 2005]*)).

4.0 Conclusions

The first complete surface velocity maps of the glaciated region of the QEI reveal a marked asymmetry in flow structure (Fig. 1), with higher rates of motion in areas of higher accumulation and deep subglacial troughs, and lower rates in regions underlain by flatter topography and lower accumulation *[Koerner, 1979]*. Velocities of land-terminating glaciers are usually restricted to velocities of ~20 - 50 m a^{-1} (interquartile range) along their main trunk, except on surge-type glaciers in their active phase. Maximum velocities of tidewater-

terminating glaciers are ~30 – 90 m a^{-1} (interquartile range) along their main trunks and typically rise to <300 m a^{-1} at their termini. Total dynamic mass losses are currently 2.6 ± 0.8 Gt a^{-1}, about half of which is drained through the Trinity and Wykeham Glaciers of POW Icefield. Although the QEI contains ~25% of Arctic glacier ice outside the Greenland Ice Sheet, it contributes only ~7.1% of the total reported dynamic ice discharge from GIC in the circumpolar Arctic (excluding Greenland). This is largely a function of the QEI's continental climate and lower rate of mass turnover compared to other Arctic regions, together with the fact that large regions of many QEI ice masses terminate on land.

Our results suggest that mass loss by surface melt and runoff currently dominates the loss term in the mass balance of the QEI, and that ice discharge has become a proportionally smaller component of that term in recent years. However, changes in tidewater glacier dynamics due to the termination or initiation of surges can rapidly change the rates at which ice is transported to the oceans from the QEI. For example, the 2003 surge of the Mittie Glacier likely increased total regional ice fluxes by ~35%. This oscillation between faster and slower flow necessitates continued annual mapping of ice motion in order to identify all surge-type glaciers in the QEI and quantify the impact of surge cycles on glacier mass balance. Further studies are also required to understand seasonal and long-term variations in motion on non surge-type glaciers in the QEI.

Acknowledgements:
We thank NSERC, Canada Foundation for Innovation, Ontario Research Fund, ArcticNet, Ontario Graduate Scholarship, University of Ottawa and the NSERC Canada Graduate Scholarship for funding. RADARSAT-2 data were provided by MacDonald, Dettwiler and Associates under the RADARSAT-2 Government Data Allocation administrated by the

Canadian Space Agency. Support to DB is provided through the Climate Change Geosciences Program, Earth Sciences Sector, Natural Resources Canada (ESS Contribution #20130293). We also acknowledge support from U.K NERC for grants GR3/12469 and NE/K004999 to JAD.

5.0 References:

Arendt, A., T. Bolch, J.G. Cogley, A. Gardner, J.O. Hagen, R. Hock, G. Kaser, W.T. Pfeffer, G. Moholdt, F. Paul, V. Radić, L. Andreassen, S. Bajracharya, N. Barrand, M. Beedle, E. Berthier, R. Bhambri, A. Bliss, I. Brown, E.Burgess, D. Burgess, F. Cawkwell, T. Chinn, L. Copland, B. Davies, H. De Angelis, E. Dolgova, K. Filbert, R. Forester, A. Fountain, H. Frey, B. Giffen, N. Glasser, S. Gurney, W. Hagg, D. Hall, U.K. Haritashya, G. Hartmann, C. Helm, S. Herreid, I. Howat, G. Kapustin, T. Khromova, C. Kienholz, M. Koenig, J. Kohler, D. Kriegel, S. Kutuzov, I. Lavrenti ev, R. LeBris, J. Lund, W. Manley, C. Mayer, E. Miles, X. Li, B. Menounos, A. Mercer, N. Moelg,P. Mool, G. Nosenko, A. Negrete, C. Nuth, R. Pettersson, A. Racoviteanu, R. Ranzi, P. Rastner, F. Rau, B. Raup, J. Rich, H. Rott, C. Schneider, Y. Seliverstov, M. Sharp, O. Sigurðsson, C. Stokes, R. Wheate, S. Winsvold, G. Wolken, F. Wyatt, N. Zheltyhina. (2012), Randolph Glacier Inventory [v3.0]: A Dataset of Global Glacier Outlines. Global Land Ice Measurements from Space, Boulder Colorado, USA. Digital Media.

Blaszczyk, M., J.A. Jania, and J.O. Hagen (2009), Tidewater glaciers of Svalbard: Recent changes and estimates of calving fluxes, Pol. Polar Res., 30(2), 85-142.

Braithwaite, R.J. (2005), Mass balance characteristics of arctic glaciers, Ann. Glaciol., 42(1), 225-229.

Burgess, D. O., M. Sharp, D.W.F. Mair, J.A. Dowdeswell, and T.J. Benham (2005), Flow dynamics and iceberg calving rates of Devon Ice Cap, Nunavut, Canada, J. Glaciol. 51(173), 219-230.

Burgess, E.W., R. R. Foster, and C. F. Larsen (2013), Flow velocities of Alaskan glaciers, Nat. Commun., 4(2146), 1-8, doi: 10.1038/ncomms3146.

Copland, L., M. Sharp, P. Nienow and R. Bingham (2003a), The distribution of basal motion beneath a High Arctic polythermal glacier, J. Glaciol., 49(166), 407-414.

Copland, L., M. Sharp, and J.A. Dowdeswell (2003b), The distribution and flow characteristics of surge-type glaciers in the Canadian High Arctic, Ann. Glaciol., 36, 73-81.

Dowdeswell, J.A., T.J. Benham, M.R. Gorman, D.O. Burgess, and M. Sharp (2004), Form and flow of the Devon Island ice cap, Canadian Arctic, J. Geophys. Res., 109,F02002, doi:10.1029/2003JF000095.

Dowdeswell, J.A., T.J. Benham, T. Strozzi, and J.O. Hagen (2008), Iceberg calving flux and mass balance of the Austfonna ice cap on Nordaustlandet, Svalbard, J. Geophys. Res., 113, F03022, doi:10.1029/2007JF000905.

Gardner, A. S., M. Moholdt, B. Wouters, G.J. Wolken, D.O. Burgess, M. Sharp, J.G. Cogley, C. Braun and C. Labine (2011), Sharply increased mass loss from glaciers and ice caps in the Canadian Arctic Archipelago, Nature, 473(7347), 357–360, doi: 10.1038/nature10089.

Glazovsky, A. and Y. Macheret (2006), Eurasian Arctic.in, Glaciation in north and central Eurasian in present time [in Russian with English Translation], editied by V.M., Kotlyakov,

97-114 and 438-445, Nauka, Moscow.

Gogineni, P. (2012), Radar Depth Sounder Data Products, Lawrence, Kansas, USA. Digital media. http://data.cresis.ku.edu/

Gray, A.L., N., Short, K.E. Mattar, and K.C. Jezek (2001), Velocities and flux of the Filchner Ice Shelf and its tributaries determined from speckle tracking interferometry, *Can. J. Remote. Sens.,* 27(3), 193–206.

Harbor, J.M. (1992), Numerical modelling of the development of U-shaped valleys by glacier erosion, Geol. Soc. Am. Bull., 104(10), 1364-1375, doi:10.1130/0016-7606(1992)104<1364:NMOTDO>2.3.CO;2.

Hattersley-Smith, G. (1969), Recent observations on the surging Otto Glacier, Ellesmere Island, Can. J. Earth Sci., 6(4), 883–889, 10.1139/e69-090

Herdes, E., L. Copland, B. Danielson, and M. Sharp (2012), Relationships between iceberg plumes and sea-ice conditions on northeast Devon Ice Cap, Nunavut, Canada, Ann. Glaciol, 53(60), 1-9, doi: 10.3189/2012AoG60A163.

Koerner, R. M. (1979), Accumulation, ablation, and oxygen isotope variations on the Queen Elizabeth Island Ice Caps, Canada, J. Glaciol*,* 22(86), 25-41.

Koerner, R. M. (2005), Mass balance of glaciers in the Queen Elizabeth Islands, Nunavut, Canada, Ann. Glaciol., 42(1), 417–423, doi:10.3189/ 172756405781813122.

Lenaerts, J.T.M., J.H. van Angelen, M.R. van den Broeke, A.S. Gardner, B. Wouters, and E. van Meijgaard (2013), Irreversible mass loss of Canadian Arctic Archipelago glaciers, Geophys. Res. Lett., 40(5), 870-874, doi:10.1002/grl.50214.

Mair, D., D.O. Burgess, M. Sharp, J.A. Dowdeswell, T. J. Benham, S. Marshall and F. Cawkwell (2009), Mass balance of the Prince of Wales Icefield, Ellesmere Island, Nunavut, Canada, J. Geophys. Res., 114F02011, doi:10.1029/2008JF001082.

Moholdt, G., T. Heid, T., Benham, J.A. Dowdeswell (2012), Dynamic instability of marine-terminating glacier basins of Academy of Sciences Ice Cap, Russian High Arctic, Ann. Glaciol., 53(60), 193-201, doi: 10.3189/2012AoG60A117.

Mortimer, C. A., L. Copland, and D. R. Mueller (2012), Volume and area changes of the Milne Ice Shelf, Ellesmere Island, Nunavut, Canada, since 1950, J. Geophys. Res., 117F04011, doi:10.1029/2011JF002074.

Müller, F. (1969), Was the Good Friday Glacier on Axel Heiberg Island surging?, Can. J. Earth Sci., 6(4), 891-894, doi: 10.1139/e69-091.

Narod, B. B., G.K.C. Clarke, and B.T. Prager (1988), Airborne UHF sounding of glaciers and ice shelves, northern Ellesmere Island, Arctic Canada, Can. J. Earth Sci., 25(1), 95–105, doi: 10.1139/e88-010.

Ommanney, C.S.L. (1969), A study in glacier inventory: the ice masses of Axel Heiberg Island, Canadian Arctic Archipelago, Axel Heiberg Island Research Reports ,McGill

University, Montreal, Canada.

Paterson, W.S.B. (1994), The physics of glaciers, third edition,Elsevier, Oxford.

Raymond, C.F. (1983), Deformation in the vicinity of ice divides, J. Glaciol., 29(103), 357-373.

Sharp, M., D. O. Burgess, J. G. Cogley, M. Ecclestone, C. Labine, and G. J. Wolken (2011), Extreme melt on Canada's Arctic ice caps in the 21st century, Geophys. Res. Lett., 38, L11501, doi:10.1029/2011GL047381.

Short, N. H. and A. L. Gray (2004), Potential for RADARSAT-2 interferometry: glacier monitoring using speckle tracking, Can. J. Remote Sens., 30(3), 504-509, doi: 10.5589/m03-071.

Short, N. H. and A.L. Gray (2005), Glacier dynamics in the Canadian High Arctic from RADARSAT-1 speckle tracking, Can. J. Remote Sens., 31(3), 225–239, doi: 10.5589/m05-010.

Van Wychen, W., L. Copland, L. Gray, D. O. Burgess, B. Danielson, M. Sharp (2012), Spatial and temporal variation of ice motion and ice flux from Devon Ice Cap, Nunavut, Canada, J. Glaciol., 58(210), 657–664, doi: 10.3189/2012JoG11J164.

Williamson, S., M. Sharp, J. Dowdeswell, and T. Benham (2008), Iceberg calving rates from northern Ellesmere Island ice caps, Canadian Arctic, 1999-2003, J. Glaciol., 54(186), 391-400.

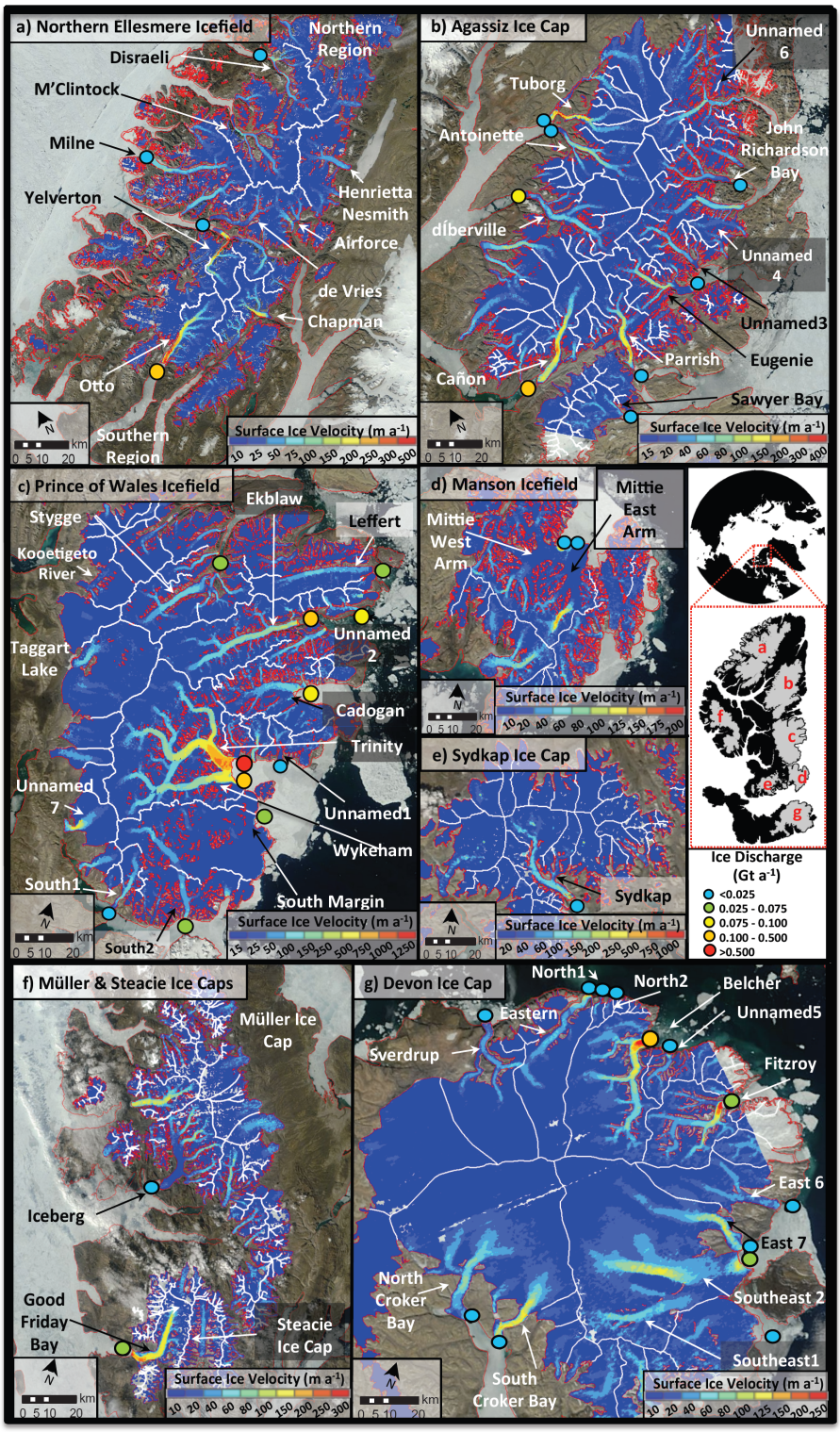

Figure 1: *Surface velocities for: a) Northern Ellesmere Icefield; b) Agassiz Ice Cap; c) Prince of Wales Icefield; d) Manson Icefield; e) Sydkap Ice Cap; f) Müller and Steacie Ice Caps; g) Devon Ice Cap. Major ice divides used to determine errors denoted in white. Note difference in velocity scale between images, although ice discharge scale remains constant (Base Image: MODIS July 4th, 2011). Inset Map: Study Site.*

Table 1: Pan-Arctic comparison of ice discharge estimates.

Region		Period	Ice Discharge (Gt a^{-1})	% of Pan-Arctic Discharge (excluding Greenland)	Data Source
CAA	Queen Elizabeth Islands	2012	2.46	7.1	This Study
	Baffin & Bylot Islands	1999-2003	0.25	0.7	Gardner et al., [2011]
Alaska	All Glaciers	2006-2010	17.1	49.7	Burgess et al., [2013]
Russia	Academy of Sciences Ice Cap	2003-2009	1.4	4.1	Moholdt et al., [2012]
	Franz-Josef Land	1952-2001	4.3	12.5	Glazovsky and Macheret [2006]
	Novaya Zemlya	1952-2001	1.4	4.1	Glazovsky and Macheret [2006]
	Severnaya Zemlya	1952-2001	0.75	2.2	Glazovsky and Macheret [2006]
Svalbard	All Glaciers	2000-2006	6.75	19.6	Blaszczyk et al., [2009]
Pan-Arctic Glaciers and Ice Caps (excluding Greenland)			34.41	100	